# Three-dimensional breast cancer spheroids for preclinical assessment

## Physical characterization of breast cancer spheroids using GrowDex as scaffolds

Ayesha Bhairo

Delft University of Technology

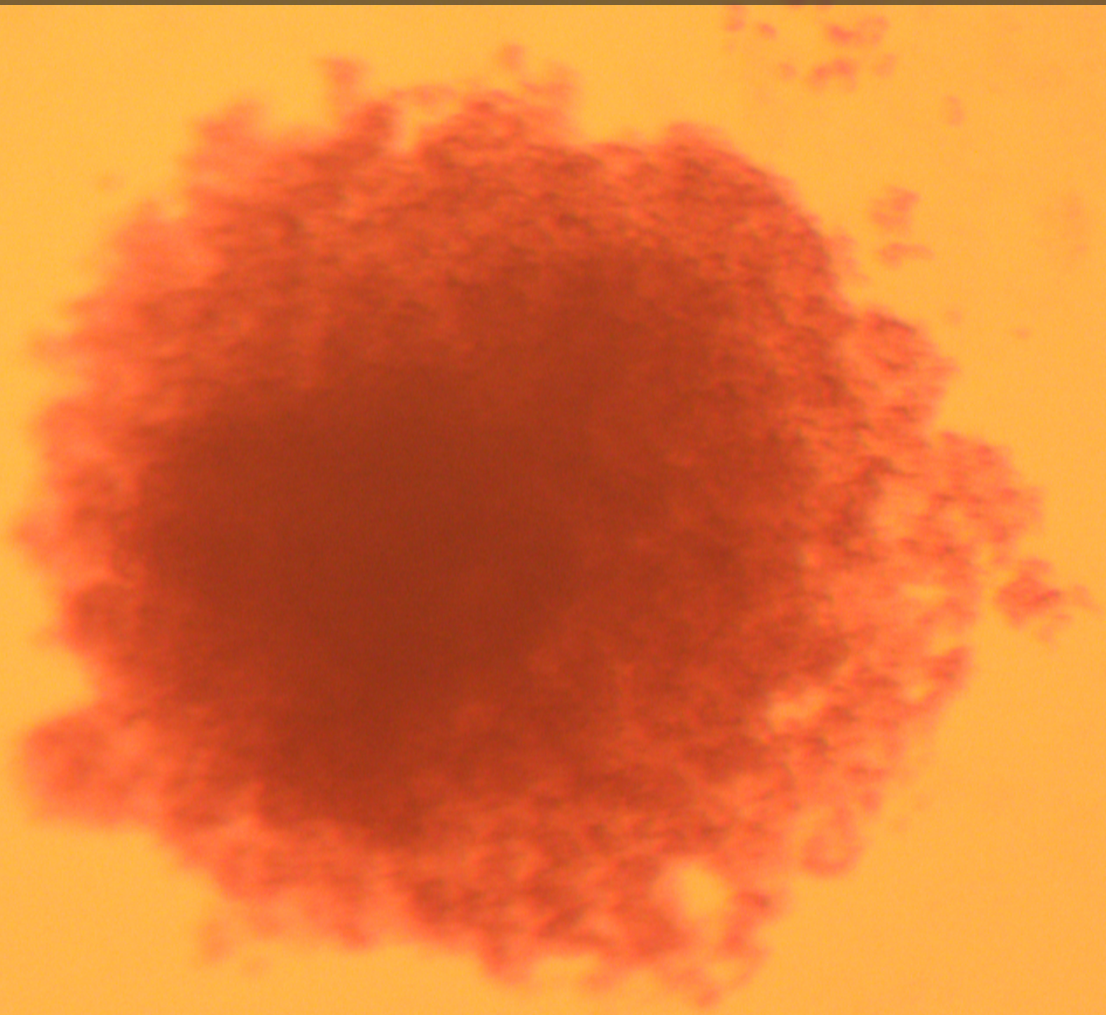

TU Delft

# Three-dimensional breast cancer spheroids for preclinical assessment

## Physical characterization of breast cancer spheroids using GrowDex as scaffolds

by

Ayesha Bhairo

To obtain the degree of Bachelor of Science
at the Delft University of Technology,
to be defended publicly on Monday July 14, 2022 at 13:00 .

Student number: 4540808
Project duration: April 11, 2022 – July 14, 2022
Thesis committee: Dr. K. Djanashvili, TU Delft, supervisor
Dr. ir. A. Denkova, TU Delft
Dr. R. A. Nadar, TU Delft

TU Delft

# Summary

Breast cancer is one of the most dangerous forms of cancer worldwide. Continuous research is therefore essential in order to find realistic treatment options. 3D tumor spheroids have been proven to imitate the structural and physiological TME of *in vivo* tumors relatively more accurate than the more widely used 2D cell cultures.

During this study, the aim was to find the optimal conditions for single spheroid formation, employing breast cancer cells and utilizing GrowDex. Different concentrations and cell densities were used, as well as differing methods (GrowDex addition prior or (days) after cell cluster formation). The liquid overlay technique was used to grow the spheroids, which were observed for a maximum of 14-16 days. Finally, an ATP viability assay was performed to determine whether the spheroids contained a proliferation zone, which corresponds to active cells.

Single spheroids were obtained for all cell densities. The relatively high GrowDex concentrations responded well to a cell density of 2000 cells, while the relatively low GrowDex concentrations responded well to cell densities of 5000 and 10000 cells. Through the ATP viability assay the samples illustrated the presence of a proliferation zone, and thus active cells.

# Contents

# Nomenclature

## Abbreviations

| Abbreviation | Definition |
|---|---|
| 3D | Three-dimensional |
| HER2 | Human epidermal growth factor receptor 2 |
| ER | Estrogen receptor |
| PR | Progesterone receptor |
| TME | Tumor microenvironment |
| ECM | Extracellular matrix |

# 1 Introduction

## 1.1. General

According to a study by the World Cancer Research Fund (2020), breast cancer is the most common and deadly form of cancer among women, and ranks in the top three commonly occurring cancers overall [1][2][3]. Mortality rates have increased globally in the past twenty-five years, with Latin-America and the Caribbean projecting the biggest increase. In contrast, most developed countries portrayed a decline in mortality rates [2]. This decline can mainly be attributed to efficient therapy, but more importantly, early detection methods, as breast cancer is curable in 70-80% of the cases as long as it is in an early, non-metastatic stage [2][4][3]. Once metastasized and spread to other organs, it is considered incurable with current therapies [3].

Breast cancer is a proliferation of cells that can outwardly be observed as lumps where the cancer is present [1]. On a molecular level, it is a heterogeneous disease featuring the activation of the HER2 protein, the hormone receptors ER and PR, as well as BRCA[1] mutations [3]. While originating in the breast area, it can spread to other parts of the body through lymph-, and blood vessels [1]. The lymph nodes can actually be used to monitor metastasis. For example, finding cancer cells in the lymph nodes close to the original tumor may indicate the cancer to be in an early stage, as it has not spread (much) beyond its primary area [6].

Seven main forms of breast cancer have been identified, each requiring a cocktail of treatment options. These treatment options are based on the molecular subtype of the cancer, and can be divided into locoregional and systemic treatments. Locoregional therapies include surgery and radiation therapy. Systemic therapies include endocrine therapy[2], chemotherapy, anti-HER2 therapy[3], bone stabilizing agents, poly(ADP-ribose) polymerase inhibitors[4] and recently, immunotherapy [5].

Breast cancer research is essential for new discoveries and improvements on conventional therapies [7]. Especially for triple negative breast cancers, which are defined by their lack of ER, PR, and the HER2 protein, resulting in the cells testing negative thrice [8]. This type of breast cancer is estimated to only account for 10% of all breast cancer types [9][8]. Nevertheless, it is a highly aggressive form of cancer, associated with poor survival chances, and high risks of metastasis and recurrence. Furthermore, the lack of the aforementioned receptors limit treatment options, with chemotherapy being the most common [7][10][11].

## 1.2. Research objective

*In vivo* solid tumor growth occurs within a 3D tissue microenvironment, with the cells in constant contact with the ECM and stromal cells[5]. Therefore, 3D cell cultures better imitate the TME[6] than 2D cultures,

[1] Tumor suppressor genes responsible for proteins to repair damaged DNA. Pathogenic variants of these genes can cause cancer [5]

[2] For hormone receptor-positive disease [5]

[3] For HER2-positive disease [5]

[4] For BRCA mutation carriers [5]

[5] Macrophages and fibroblasts

[6] Complex ecosystem responsible for the tumors' survival and response to treatment [12]

due to the cell-cell interactions as well as the cell-matrix interactions that are possible [11]. Failure to correctly model and analyze realistic tumor growth can lead to expensive studies with inaccurate conclusions [13]. Naturally, the biggest challenge in preclinical studies involves the accurate simulation of the TME [11][12][14][15][16][17]. The advancement of tissue engineering as a biomimetic approach offers promising insights for the screening of anticancer therapeutics by using *in vitro* tumor models, like spheroids[7], to simulate the *in vivo* microenvironment [12][14][16][18]. Remarkably, this technique produces a realistic treatment response because it imitates a relatively accurate portrayal of the 3D structure of the cancer cells as well as the TME.

Wishart et al. (2021) argued 3D spheroid cultures also account for the *in vivo* conditions like the hypoxic regions, pH, and metabolic gradients that are of importance during treatment [12]. Compared to 2D cell cultures, 3D spheroid models better imitate the features of *in vivo* tumors *ex vivo*, including that of drug resistance and the effects of radiation and hyperthermia [14][16][17]. Brüningk et al. (2020) predicted 3D tumor spheroids to respond to heat and radiation treatments in such a way that is not perceptible in 2D cell cultures, but which may influence treatment efficacy [17]. Although the 3D spheroids do not own vasculature and cellular heterogeneity that are of importance during mutations and clonal evolution, the 3D molecular structures more accurately mimic those of patient tumors than do 2D models [17]. By making use of this 3D cell culture technique, potentially effective prototypes can be identified during the preclinical development stage, preventing failures in an early stage.

Currently, multiple tumor spheroids are gaining increased recognition for their biological relevance [19]. However, the formation of singular spheroids is difficult, as most tumor cell lines form loose aggregates in 3D [20]. Especially for breast tumor spheroids, protocols are inconsistent [21]. Froehlich et al. (2016) compared different techniques, cell densities, and additives to generate spheroids. Their results illustrate breast cancer cells to mainly form loose aggregates and/or multiple (small) spheroids [21]. However, the formation of singular spheroids is useful when closely observing the effects of cancer therapies like radiation or heat treatment.

There is a wide variety of techniques for growing 3D spheroids [22]. However, the amount of information on the methodology of growing spheroids using GrowDex, an animal-free hydrogel with a completely known composition, is rather limited. Therefore, this study aims to find the optimal conditions for single spheroid formation, employing breast cancer cells and utilizing GrowDex, for preclinical assessment.

## 1.3. Approach

This study will make use of the triple negative MDA-MB-231 breast cancer cell line. GrowDex dilutions will be used to form single spheroids. In order to test the viability of the cells, an ATP viability assay will be performed.

[7] Three-dimensional aggregation of cells [18]

# 2

# Theoretical background

## 2.1. MDA-MB-231 cell line

The BRCA1 and BRCA2 genes are tumour suppressor genes associated with breast cancer. Women with loss-of-function mutations in the BRCA1 or BRCA2 genes most commonly develop triple negative breast cancers [9].

The human epithelial breast cancer cell line MDA-MB-231, derived from a 51-year-old caucasian woman, is not only triple negative, but has a mutated p53 (tumor suppressor) gene [9][10]. Much like other invasive cancer cell lines, its invasiveness is caused by the degradation of the ECM [10]. MDA-MB-231 accurately portrays late stage triple negative breast cancer, and is commonly used for medical research [9][10].

## 2.2. Conventional preclinical models

Conventional *in vivo* experiments utilize animals (xenografts) to simulate a realistic TME. Xenografts are primarily used for the monitoring of drug bioavailability, therapeutic efficacy, and dose-limiting toxicity [14]. However, these methods possess certain limitations that hinder the importance to humans, i.e., foreign physiology due to transplantation of human cells into mouse models, limited heterogeneity, and reduced tumor mutation rates [12][14]. Moreover, as animal models heavily impact the lives of the animals involved, its relation to tumor research is highly controversial, expensive and time-consuming [12][14][23].

Preclinical *in vitro* studies on the other hand, commonly involve 2D cell cultures where cells grow in a monolayer [12][14]. This simplistic and cost-effective method has caused a reduction in the use of laboratory animals [12][16]. However, this method cannot epitomize certain essential features of the TME (i.e. structure, cell-matrix-, and cell-cell interactions) that contribute to the complexity and orientation of the human body. The monolayer implicates that cell seeding needs to be done on polystyrene surfaces (i.e. petri dishes) which causes the cells to stretch out across the culture medium. The resulting increase in area ensures the tumor cells have easy access to oxygen and nutrients, contrary to the physiological TME where there is an inhomogeneous supply of oxygen and nutrients characteristic for live tissue [17] (Figure 2.1). From figure 2.1 it is clear that the inner cells of 3D cultures do not interact as well with oxygen and nutrients as do 2D cultures. Furthermore, the limited amount of neighboring cells result in a reduction of intercellular communication [14][16][17]. A more realistic option would be to use 3D cell cultures (Figure 2.1).

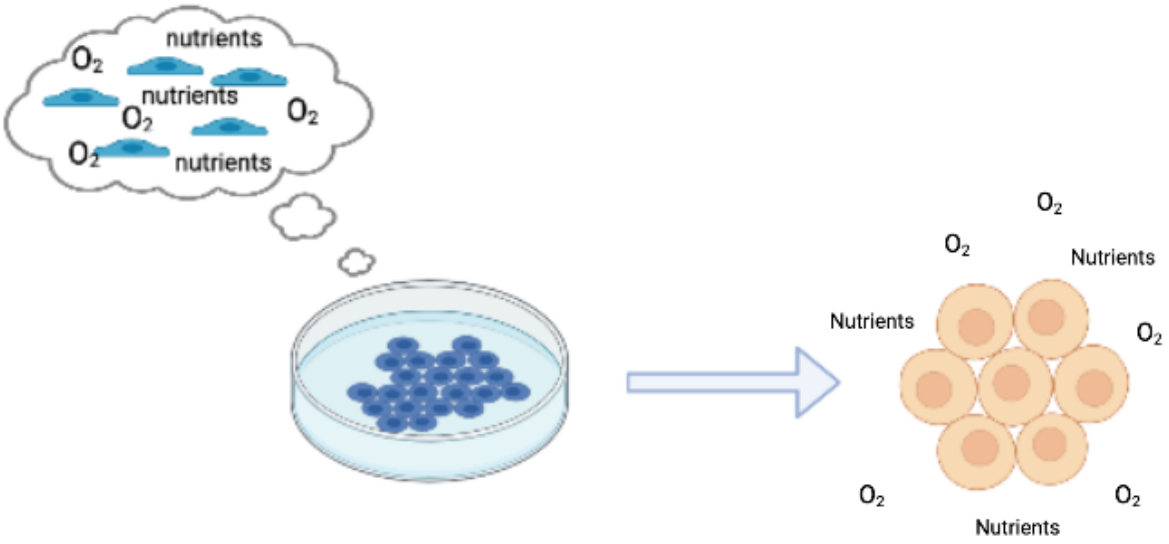


**Figure 2.1:** Cell seeding on a petri dish illustrating the easy access of oxygen and nutrients. 3D cell cultures better imitate the physiological TME and its inhomogeneous supply of oxygen and nutrients. [Created with BioRender]

The application of 3D biopsied tumor tissues offers a solution, as it holds a more realistic approach to imitating *in vivo* conditions [18]. Biopsied tumor tissues have mostly been used for diagnostic purposes but can be utilized for *ex vivo* drug testing as well. Unfortunately, acquiring sufficient biopsied material has proven difficult. But the most important drawback is that surgical removal causes biopsied tissue to undergo oxygen and nutrient depletion as well as temperature and mechanical stresses. This causes 3D biopsied tissue samples to have a deficit in reproducibility [18].

Other methods exist for assembling 3D cultures *in vitro*. In order to mimic the cellular microenvironment, two main techniques can be categorized. The first makes use of scaffold-based 3D cell cultures, where the cells are anchored to 3D platforms consisting of either natural (i.e. collagen), synthetic (i.e. polycaprolactone), or semi-synthetic (i.e. chitosan) biomaterials that imitate the cellular microenvironment [16]. This technique is often paired with other technologies [16][24][25]. For example, bioprinting is a 3D scaffold-based technique. Similar to standard 3D printing, it requires the successive printing of 2D structures to ultimately form a 3D scaffold that can be applied for tissue and organ regeneration purposes. [26][25]. This method can be combined with microfluidic technology, where micron sized fluidic channels in a polymer has tubing and pumping peripherals attached through which fluid is pumped. [25][24]. The fluid is highly controllable and the microscale dimensions make it possible to epitomize *in vivo* conditions. Moreover cell flow can be easily manipulated [25].

The second method for assembling 3D cell cultures *in vitro* is non-scaffold-based, where the cellular microenvironment consists of proteins produced by the cell itself during culture formation [16][24]. The non-scaffold-based 3D cell cultures are typically formed by spheroids. These are cellular aggregates in suspension, consisting of natural peptides and a hydrogel to support the cell-cell interaction and adhesion [12][16][17].

## 2.3. Spheroids

Spheroids are particularly interesting *in vitro* models for their ability to imitate the most important features of *in vivo* solid tumors, including cellular heterogeneity, cell-cell signaling, internal structure, and chemotaxic-driven movements. These factors strongly influence cytotoxicity assays [16][17][18]. Spheroids contain an external layer of cells with high proliferation rates because this layer has easier access to oxygen and nutrients [16][17]. Furthermore, spheroids contain a middle layer of quiescent cells, and a core of necrotic cells. Both cell types are in a hypoxic environment and have a nutrient-deficiency [16][17]. These attributes can be seen in figure 2.2.

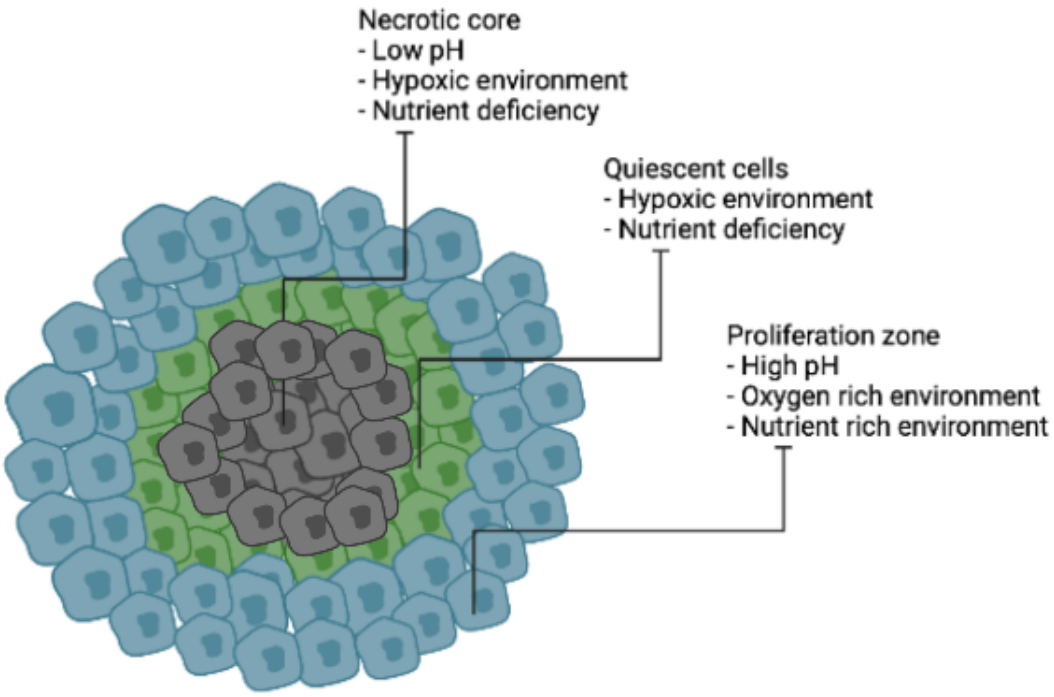


**Figure 2.2:** Internal spheroid structure, composed of a necrotic core, quiescent cells, and a proliferation zone. [Created with BioRender]

Through the absence of oxygen, cancer cells convert pyruvate into lactate to obtain energy (Warburg effect) [16]. Consequently, lactate accumulation acidifies the internal spheroid environment, similarly to the process of *in vivo* solid tumors [16]. Cell-cell and cell-ECM interactions create a physical barrier preventing penetration and distribution of anticancer therapeutics. The internal organization of spheroids hinder drug loaded nanocarriers, as well as oxygen and nutrients, due to their limited permeability and therefore impair therapeutic anticancer drug efficacy. [16][18]. Specifically, the inner layers impair the efficacy of drugs that promote cellular death via the formation of reactive oxygen species, as their environment is hypoxic (Figure 2.2) [16][18]. Furthermore, drugs with a high efficacy in rapidly dividing cells, perform poorly in the inner layers as well, due to the senescent and necrotic cells (Figure 2.2) [16]. And finally, the low pH characteristic for spheroids can alter the properties of certain drugs [16].

3D spheroid cultures are not entirely without drawbacks. For example, they require complex and expensive assays on large structures [8][11]. But more importantly, they lack robust porosity and mechanical stability, which can impair the reliability of the TME. Moreover, the necrotic core has thus far hindered the possibility of long-term studies [12]. The use of spheroid models in preclinical research studies also poses a challenge in the sense that there are currently a limited number of large-scale reproducible techniques for the formation of spheroids with uniform sizes [16]. Cell death dynamics impact spheroid growth response. 2D cell cultures have homogeneous access to nutrients and oxygen and can therefore grow exponentially and slip off the substrate when the cell dies. Contrarily, spheroid models, like tumors, are heterogeneous and contain a dynamic evolution mechanism. Therefore their microenvironment changes continually and with it, the efficacy of treatment [17]. There are several tools and techniques available to grow and characterize 3D spheroids (Table 2.1). However, the amount of research on growing spheroids with GrowDex is rather limited.

**Table 2.1:** Examples of spheroid formation techniques with their respective advantages and disadvantages

| Technique | Advantages | Disadvantages | References |
|---|---|---|---|
| Forced floating | - Simple and inexpensive<br>- Easily accessible spheroids suitable for high throughput testing | - Cell shape and size can vary when cell seeding is not fixed<br>- Laborious plate coating required | [27] |
| Hanging Drop | - Inexpensive when using 96-well plates<br>- Easily accessible homogenous spheroids suitable for high throughput testing | - Expensive when using different kind of plates<br>- Laborious plate preparation<br>- Medium exchange without disturbing cells is difficult when working with small volumes | [27] |
| Agitation-based approaches | - Simple<br>- Easily accessible spheroids<br>- Easy large scale production<br>- Nutrient transport through culture motion | - Special equipment needed<br>- No manipulation of cell number and sizes<br>- Time consuming and extra steps necessary for homogeneous spheroids<br>- Shear force exposure (spinner flasks) | [27] |
| Matrices and scaffolds | - Create 3D support that imitates in vivo conditions<br>- Growth factors present | - Expensive for large scale production<br>- Difficult to retrieve cells after 3D culture formation | [27] |
| Magnetic Levitation | - Long term research possibilities<br>- Rapid assembly of spheroids<br>- Easily accessible spheroids<br>- Scarce cell resources can be used optimally<br>- Additional cells can be added later on to preserve in vivo microenvironment | - Cost-benefit tradeoff should be considered | [28][29] |
| Microfluidic cell culture platforms | - Suitable for high-throughput screening | - Special equipment needed<br>- Extensive analysis of the 3D culture can be difficult | [27] |

For high content screening, it is important to take into account three main obstacles: the spheroid shape and size heterogeneity, staining (including imaging and analysis), and the implementation into an industrial setting. Due to depth-dependent light scattering, quantifying the fluorescent signals from spheroids prove to be challenging. Furthermore, antibodies have difficulty impenetrating whole spheroids [30]

Other solutions include the engineering of equivalently sized spheroids via technological plates (i.e. microspace cell culture plates7) that are compatible with high throughput imaging. However, this technique limits the maximum spheroid dimensions [30]

Spheroid growth kinetics can be categorized into three stages: 1) The initial growth stage, where the tumor volume increases exponentially, 2) The dormant growth stage, where cellular growth is maintained, and 3) The vascular growth stage, where ECM remodeling and secretion of angiogenic factors induce the formation of new vessels [16].

## 2.4. GrowDex

GrowDex is an animal-free hydrogel, with a completely known composition: 100% wood-derived nanofibrillar cellulose and water [31] . It can be used to support cell growth and differentiation by mimicking the extracellular matrix. GrowDex has been used in the past for 3D cell cultures in regenerative medicine and *in vivo* tumor models amongst others. As animal-derived matrices are notoriously difficult to work with, GrowDex offers numerous benefits (Table 2.2). These include the ability to translate cell culture assays into clinical applications. Animal-derived matrices like Matrigel, which is derived from mouse tumor cells, are more difficult to translate to clinical applications as they contain unknown compounds [32]. The biggest difference between GrowDex and general hydrogels is its high reproducibility, as there is no lot-to-lot variation and it is less difficult to work with [16][30].

**Table 2.2:** GrowDex vs. Animal-derived matrices [31]

| | **Growdex** | **Animal-derived matrices** |
|---|---|---|
| **Handling temperature** | Room temperature | <4°C |
| **Polarization temperature** | Not necessary | 22 - 37°C |
| **Compatible dilution solution** | Any media | Commonly PBS |
| **Stiffness tunability** | low kPa range (0 - 2000 Pa). Can be fine-tuned by diluting with culture media | Unknown |
| **Storage** | Unopened: Room temperature<br>Opened: 4 - 8 °C | -20°C |
| **Autofluorescence** | Non | Background fluorescence due to (unknown) proteins |
| **Compatible pipet tips** | Low-retention and low-adhesion | Pre-cooled (-4°C) |
| **Purity** | RNA/DNA-free | Traces of animal RNA/DNA |

## 2.5. ATP viability analysis

The cell viability of the 3D spheroids is important as it confirms whether the cells have grown together to form spheroids, as opposed to having been clustered together as dead cells. The latter option is not of use when testing treatment options. A variety of markers can be utilized to indicate whether cells are metabolically active. Common examples include measuring ATP levels, substrate reduction, and enzymatic activities that are unique to live cells [33].

Real-time Cell Viability illustrates the example of substrate reduction because a prosubstrate penetrates the cells. However, only viable cells with an active metabolism can convert the prosubstrate into a substrate for luciferase (Figure 2.3). Consequently, luciferase utilises the converted substrate in order to create a luminescent signal. This method does not require cellular lysis, meaning further experimentation can be done on the same cells [33].

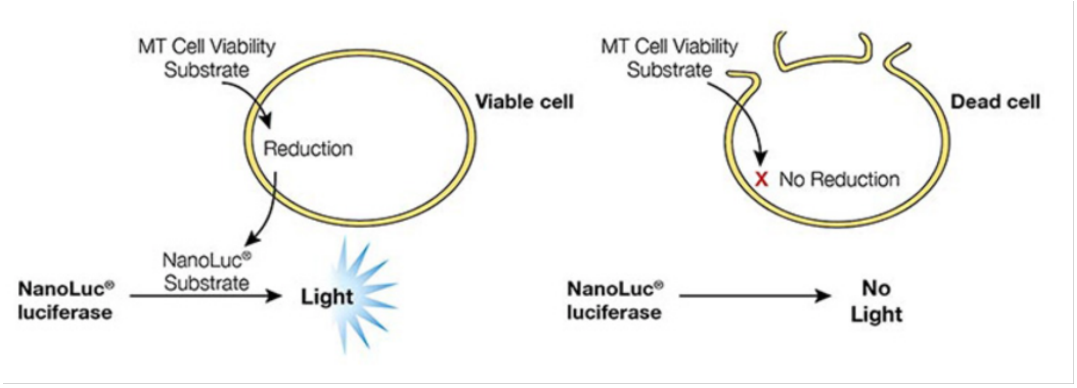


**Figure 2.3:** Real-time viability assay illustrating the ability of live cells to convert prosubstrate into a substrate for luciferase, as well as the inability of dead cells to do so [33]

An example of measuring enzymatic activities unique for live cells are Tetrazolium Reduction Viability Assays. Positively charged compounds that can penetrate viable cells, can be converted into a formazan product (Figure 2.4). During this reaction, a purple color change can be observed and therefore used as an indicator. A drawback of this technique is the long incubation time [33].

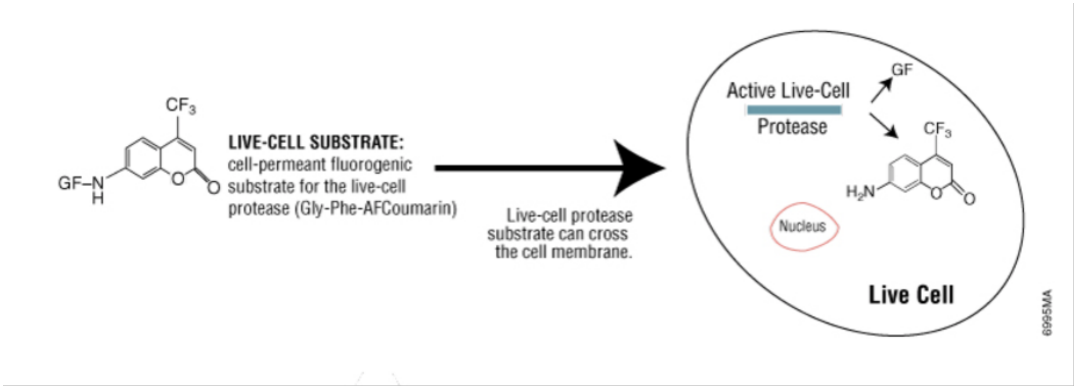


**Figure 2.4:** Tetrazolium reduction viability assay illustrating positively charged compounds to penetrate viable cells [33]

An example of measuring ATP levels is through the use of the CellTiter-Glo3D Cell viability assay. Lysis of the viable cells induce the release of ATP into the medium. Consequently, luciferase uses the released luciferin to create a luminescent signal [33]. The biggest advantage to using this type of measurment is the reduction in incubation time, as no substrate conversion is necessary [33].

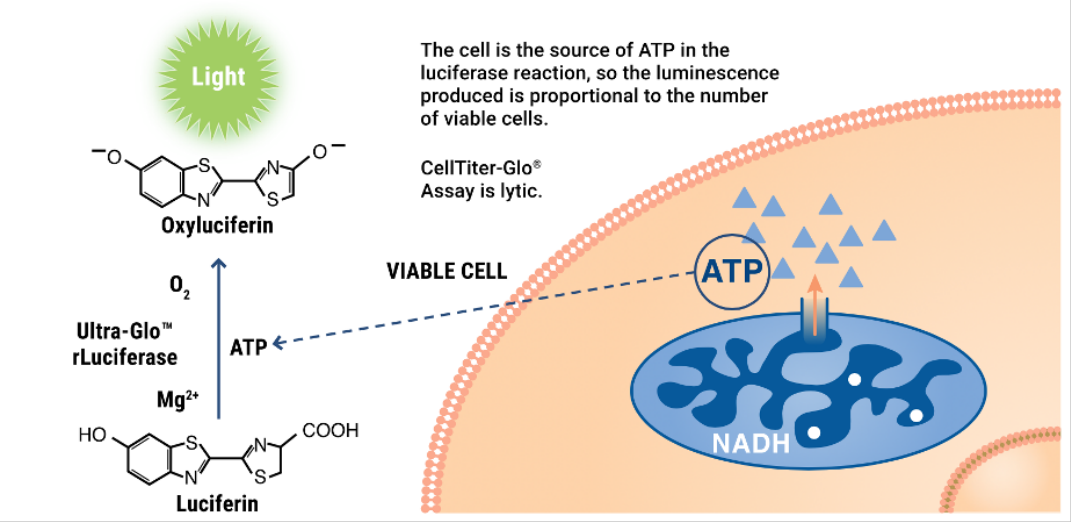


**Figure 2.5:** ATP level measurement illustrating the ability of viable cells to release ATP through cell lysis [33]

# 3

# Materials and Methods

## 3.1. Materials

The (bio)chemicals that were used during this research are as follows:

- 96% Ethanol
- DMEM high glucose (Dulbecco's Modified Eagle Medium)
- Trypsin
- FBS (Fetal Bovine Serum)
- Pen-Strep (Penicillin-Streptomycin)
- PBS (Phosphate Buffered Saline)
- MDA-MB-231 p10 breast cancer cells were obtained from the Chemical Engineering Department of the TU Delft
- GrowDex Stock (1.5%)
- CellTiter-Glo3D Cell Viability Assay

The materials that were used during this research are as follows:

- 37°C / 5%$CO_2$ Incubator (Heraeus Heracell)
- U-shaped 96-well plates
- Light microscope (Olympus Tokyo)
- Luna-II cell counter (+slides)
- Centrifuge (VWR CompactStar CS 4)
- Centrifuge (Eppendorf 5810 R)
- Fluorescence spectrophotometer

## 3.2. Method

### 3.2.1. Subculturing

Approximately twice per week, before starting an experiment, the tumor cells were subcultured in culture medium (89% DMEM, 10% FBS, and 1% Pen-Strep). This was done by first using trypsin to remove the cells from the bottom of the flask, whereafter they were resuspended in medium and centrifuged (VWR CompactStar CS 4 centrifuge). Next, the cell concentration was determined by using the Luna-II cell counter. This defined the amount of (cell) volume that had to be transferred to a new flask, which was hence incubated at 37°C / 5%$CO_2$, as well as the amount of (cell) volume required to obtain the necessary cell seeding densities of 2000, 5000, and 10000.

### 3.2.2. General approach
GrowDex contains a stock concentration of 1.5% [30]. As this solution is entirely based on cellulose, its viscosity requires dilution. Therefore, the adjustable parameters in this research are the GrowDex concentration and cell seeding density. Based on previous experiments[1] low GrowDex concentrations proved to have been a positive influence on singular spheroid formation. According to research from Froehlich et al (2016), a good way to generate breast cancer spheroids is using the liquid overlay technique (Table 2.1, forced floating). Therefore this technique was used during this research, the differing cell densities were seeded in cell-repellent U-shaped 96-well plates. GrowDex was then added either before or (days) after centrifugation with the Eppendorf 5810 R centrifuge

### 3.2.3. Experimental setup
The experiments were all carried out using cell densities of 2000, 5000, and 10000, and can be characterized into two categories:

1. Spheroid formation with 0.005 - 0.5% GrowDex (High GrowDex Concentrations, HGC)
2. Spheroid formation with 0.00001 - 0.00005% GrowDex (Low GrowDex concentrations, LGC)

GrowDex addition took place either before or (days) after cellular clustering. Spheroid kinetics were monitored until a maximum of 14-16 days.

### 3.2.4. ATP viability assay: Determining the live/dead cells
In order to quantify the live cells within the spheroids, an ATP viability assay was performed. This was done through a CellTiter-Glo3D Cell Viability Assay.

### 3.2.5. Statistical analysis
In order to accurately interpret the data, all parameters are expressed as means $\pm$ standard deviation. The statistical analyses were performed using GraphPad Prism (version 7.0) software. Two-way analysis of variance (ANOVA) with a Turkey (multiple comparisons) posthoc test was used to determine the differences among the two groups at different time points. For all statistical analysis, a value of p was considered significantly different if *p $\leq 0.05; **p \leq 0.01; ***p \leq 0.001; ****p \leq 0.0001$.

[1] Lucy van Staalduine. Establishment of three-dimensional FaDu tumor spheroids using GrowDex as scaffold. Bachelor thesis, TU Delft, 2022

# 4

# Results

### 4.0.1. Single spheroid formation using HGC

During the HGC experiments, the aim was to determine a range of relatively high GrowDex concentrations that would encourage single spheroid formation with MDA-MB-231 breast cancer cells. This was done by using a concentration range between 0.001 and 0.5% and cell densities of 2000, 5000, and 10000. GrowDex addition varied:
before (1) = immediately before cell cluster formation
after (1) = immediately after cell cluster formation
(2) = 4 days after cell cluster formation
(3) = immediately after cell cluster formation

**Cell seeding density of 2000 cells/well**

A cell seeding density of 2000 was used for GrowDex concentrations of 0.1, 0.05, 0.01, 0.005, and 0.001%. After 5-6 days, the control group went from a single spherical shaped spheroid to an irregular spheroid surrounded by a monolayer of single cells (Figure 4.1). Furthermore, figure 4.1 illustrates the higher GrowDex concentrations (0.1 and 0.05%) to generate relatively stable spheroids. They started out as singular spheroids and did not lose their shape. In contrast, low GrowDex concentrations (0.01, 0.005, and 0.001%) illustrated multiple, smaller spheroids from the start. Eventually, the spheroids broke apart and only single monolayer cells could be observed from day 7-9 on.

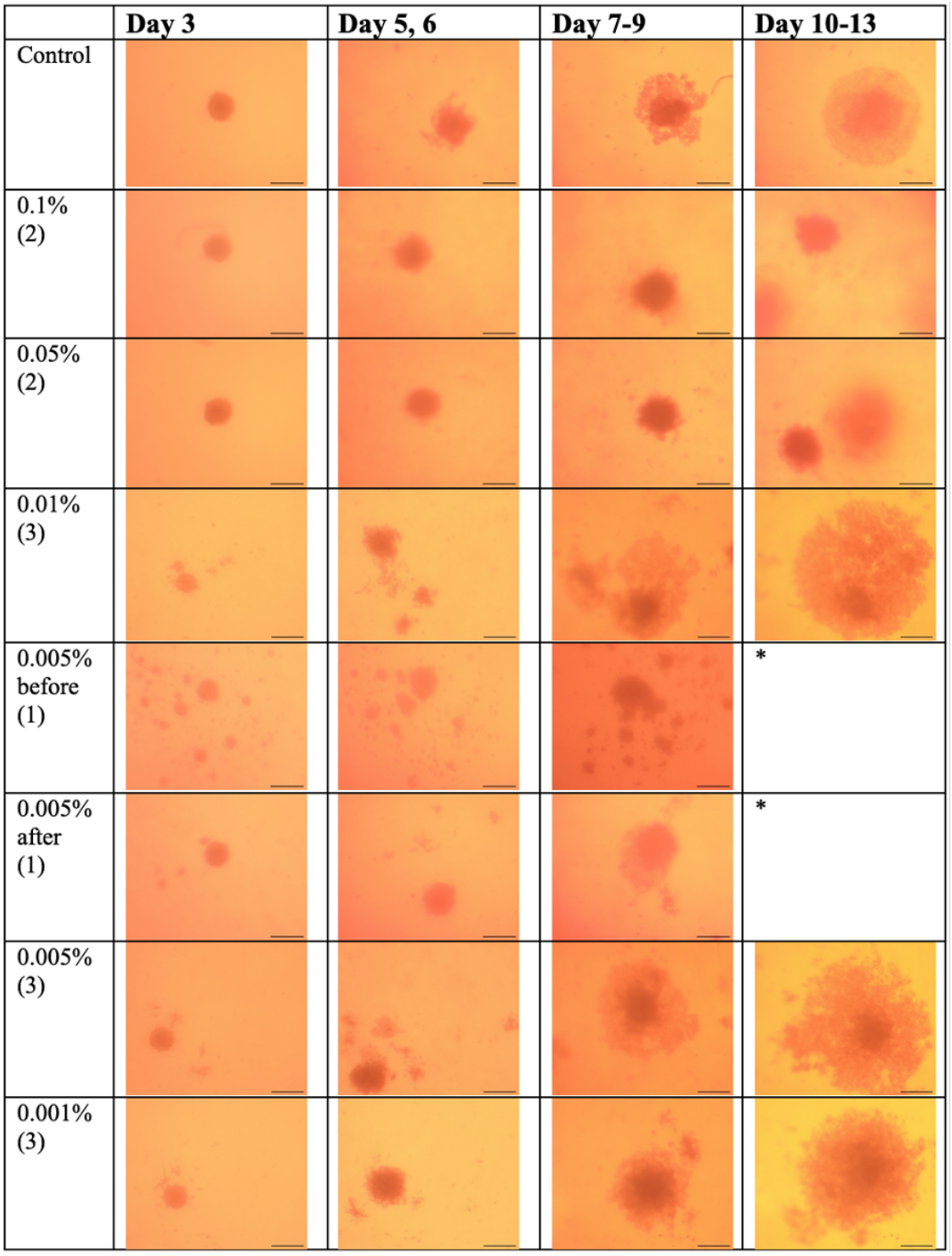


**Figure 4.1:** Differing GrowDex concentrations with a cell density of 2000 cells/well. Scale bar corresponds to 400 µm. * = contamination.

Figures 4.2 and 4.3 illustrate the growth percentages after day 3 or day 4. During the second experiment (Figure 4.2), the control group fluctuated in growth, while the control groups of the third experiment (Figure 4.3) are stable in size, with an active decrease on day 16. 0.1 and 0.05% illustrated a steady increase in growth over time. 0.001 and 0.005% illustrated an increase in spheroid size between day 6 and day 9. From day 9 to day 13 a growth plateau was observed, while an active decrease was seen from day 13-16. 0.01% illustrated irregular growth changes, but from figure 4.1 this can be attributed to the dispersion of single cells over time.

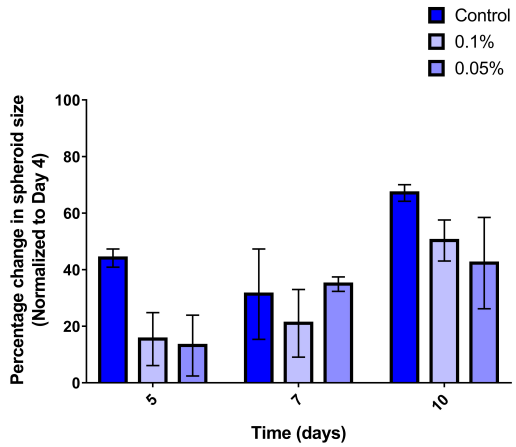


**Figure 4.2:** Relative spheroid growth rate for 2000 cell density per well with 0.1% and 0.05% GrowDex concentrations. GrowDex was added 4 days after cell cluster formation

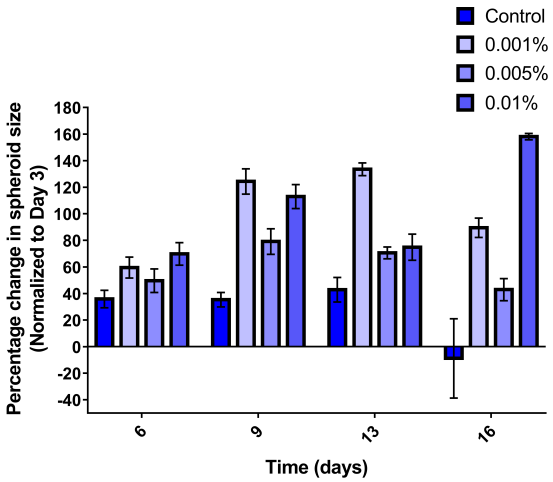


**Figure 4.3:** Relative spheroid growth rate for 2000 cell density per well with 0.01%, 0.005%, and 0.001% GrowDex concentrations. GrowDex was added 4 days after cell cluster formation

**Cell seeding density of 5000 cells/well**

A cell seeding density of 5000 was used for GrowDex concentrations of 0.5, 0.1, 0.05, 0.01, 0.005, and 0,001%. While the control group started out as a singular spheroid, a monolayer of single cells started to surround its outer boundaries around day 10 (Figure 4.4). Furthermore figure 4.4 illustrates the 0.5% (1) to encourage the formation of multiple, small spheroids. In contrast, 0.1, 0.05, and 0.01% illustrated relatively stable spheroid, as they did not change (much) in shape and no single cell monolayer could be observed. The smaller concentrations of 0.005 and 0.001% illustrated relatively stable spheroids as well, but these spheroids did show the presence a single cell monolayer.

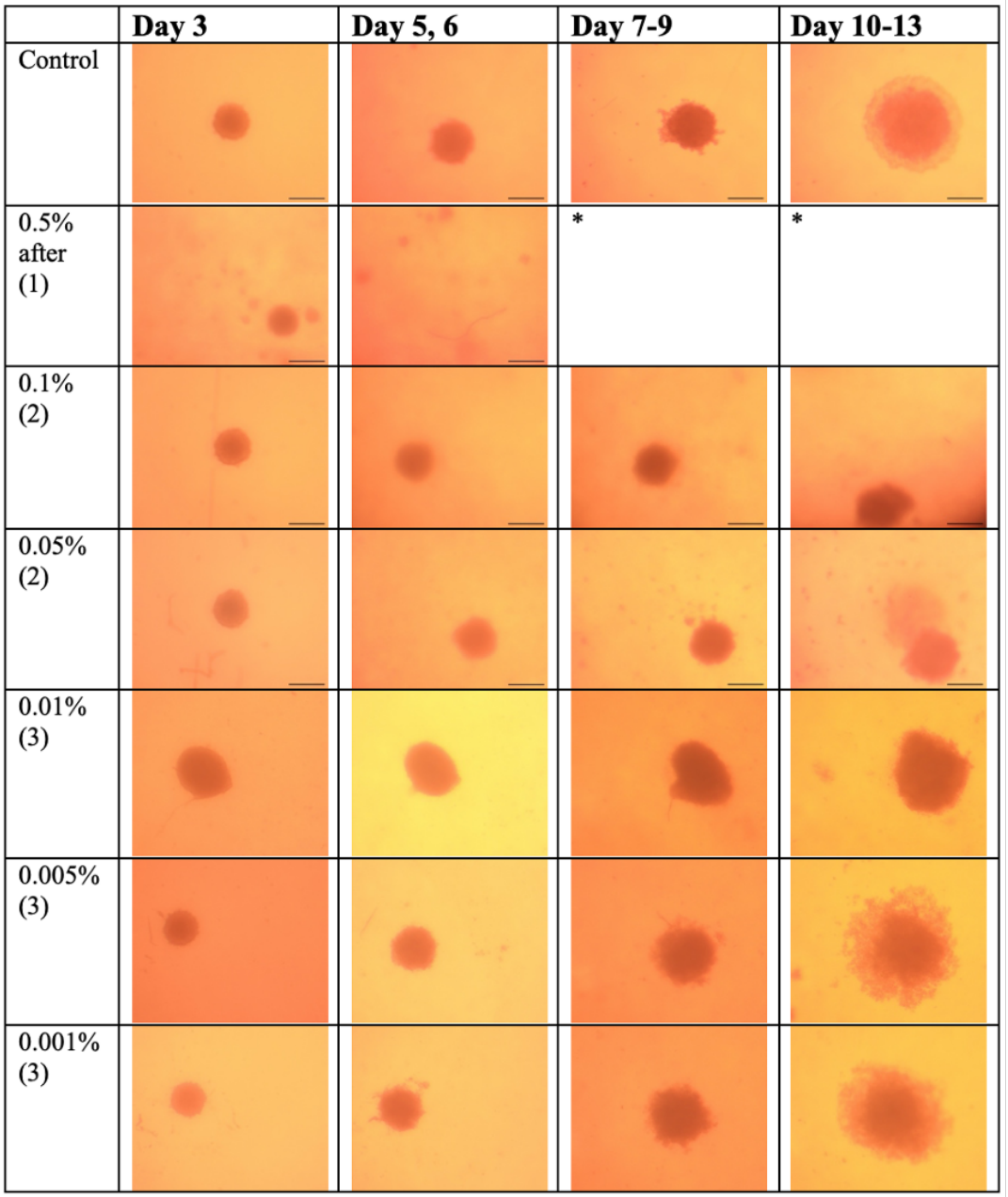


**Figure 4.4:** Differing GrowDex concentrations with a cell density of 5000 cells/well. Scale bar corresponds to 400 µm. * = contamination.

Figures 4.5 and 4.6 illustrate the growth percentages over time. In figure 4.5, the control groups illustrate an active increase in size, as does the 0.1%. Figure 4.6 illustrates that the control groups are stable in size, with an active decrease around day 16. This was already observed in figure 4.3 as the monolayer of single cells that was increasing, causing the spheroid to decrease in size. 0.001% illustrates an increase in growth at first, while becoming stagnant between day 9-13. On day 16 a decrease in growth can be observed (Figure 4.6). The concentrations of 0.005 and 0.01% illustrate an in increase in growth at first, which became a growth plateau between day 13-16.

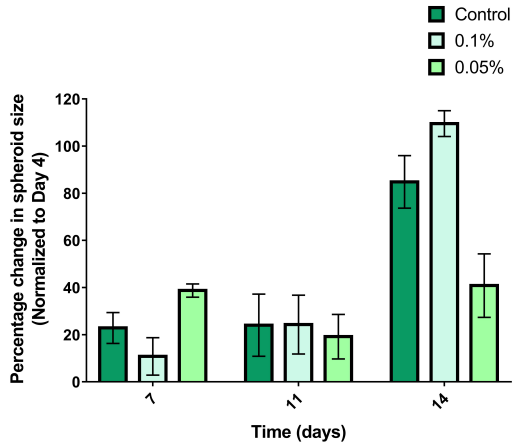


**Figure 4.5:** Relative spheroid growth rate for 5000 cell density per well with 0.1% and 0.05% GrowDex concentrations. GrowDex was added 4 days after cell cluster formation

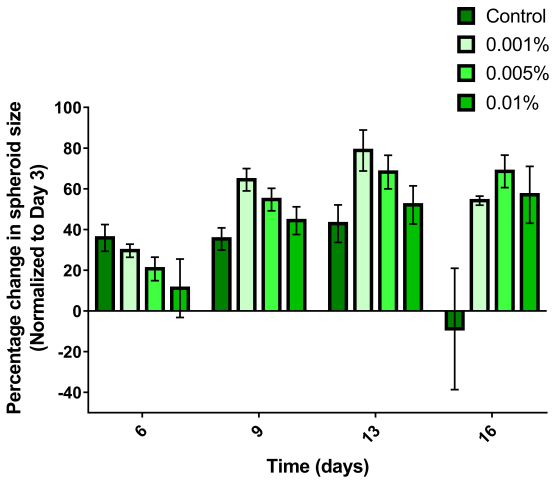


**Figure 4.6:** Relative spheroid growth rate for 5000 cell density per well with 0.01%, 0.005%, and 0.001% GrowDex concentrations. GrowDex was added 4 days after cell cluster formation

**Cell seeding density of 10000 cells/well**

A cell seeding density of 10000 was used for GrowDex concentrations of 0.1, 0.05, 0.01, 0.005, and 0.001% . Initially starting out as a single spheroid, the control group illustrated irregular shapes from day 7 onwards (Figure 4.7). In contrast, figure 4.7 illustrates all the GrowDex concentrations to form relatively stable spheroids that do not change in shape, nor contain a monolayer of single cells

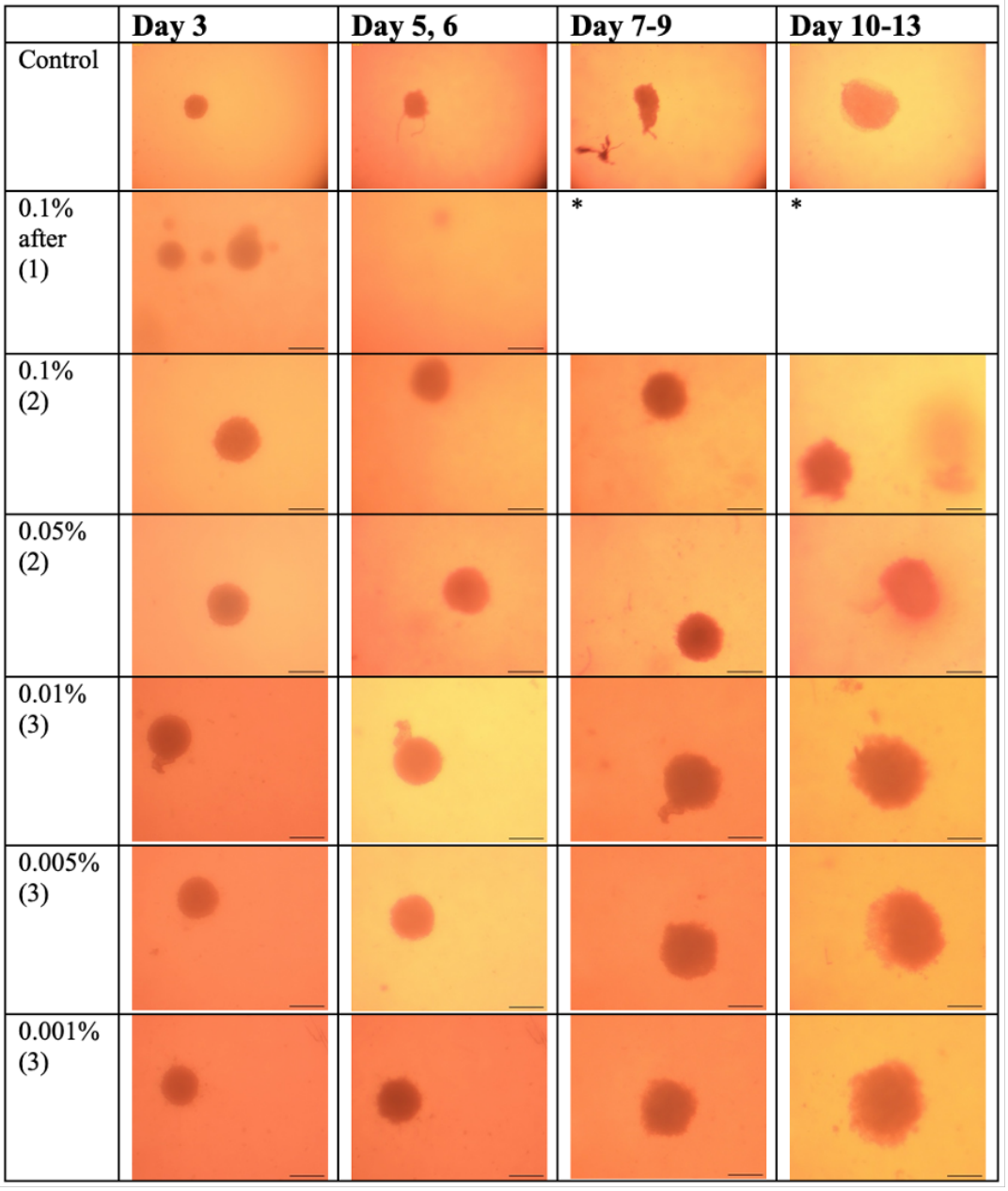


**Figure 4.7:** Differing GrowDex concentrations with a cell density of 10000 cells/well. Scale corresponds to 400 µm.* = contamination

Figures 4.8 and 4.9 illustrate the growth percentages over time. In the second experiment (Figure 4.8), the control group is illustrated to increase, while the control group of the third experiment (Figure 4.9) illustrates a decrease in spheroid growth. 0.1 and 0.05% illustrate small increase in growth (Figure 4.8). 0,001, 0.005, and 0.01% initially illustrate an increase in growth, eventually reaching a plateau growth state (Figure 4.9).

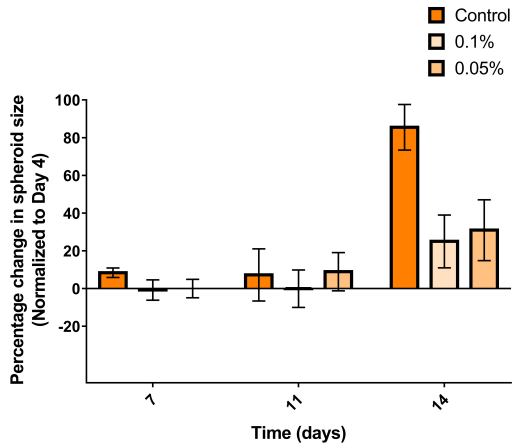


**Figure 4.8:** Relative spheroid growth rate for 10000 cell density per well with 0.1% and 0.05% GrowDex concentrations. GrowDex was added 4 days after cell cluster formation

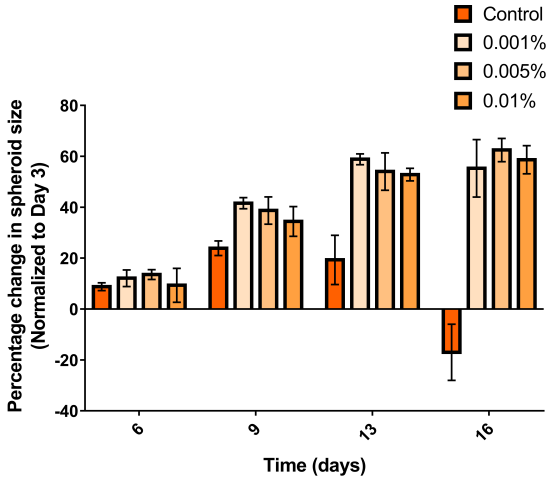


**Figure 4.9:** Relative spheroid growth rate for 10000 cell density per well with 0.01%, 0.005%, and 0.001% GrowDex concentrations. GrowDex was added 4 days after cell cluster formation

## 4.0.2. Single spheroid formation using LGC

The results from the HGC experiments, illustrated the 2000 cell density to respond better to higher concentrations of GrowDex (0.1 and 0.05%), when GrowDex was added 4 days after cell clustering. The 5000 cell density responded well to all the GrowDex concentrations (0.1, 0.05, 0.01, 0.005, and 0,001%) except for the 0.5%, regardless of addition prior or after cluster formation. The 10000 cell density responded well to all the GrowDex concentrations (0.1, 0.05, 0.01, 0.005, and 0.001%) regardless of being added before or after the cell clustering.

As the higher cell densities of 5000 and 10000 responded well to all the different concentrations, but with the lowest concentrations illustrating the biggest growth increase, even lower concentrations of 0.0005 and 0.0001% were used to better observe single spheroid formation. GrowDex addition varied:
top = cells were intentionally disturbed
bottom = cells were not (or minimally) disturbed

**Cell seeding density of 2000 cells/well**

On using a cell density of 2000 cells/well, the control group demonstrated similar behavior as the previous control groups. Initially, they illustrated single spheroids, however, over time a monolayer of single cells could be observed around the spheroids. This monolayer increased over time (Figure 4.10). Figure 4.10 illustrates that there is no difference between adding GrowDex without disturbing the cells, or adding GrowDex while minimally disturbing the cells. Furthermore, only a concentration of 0.0005% illustrated relatively stable spheroids, as all the other samples displayed a monolayer of single cells.

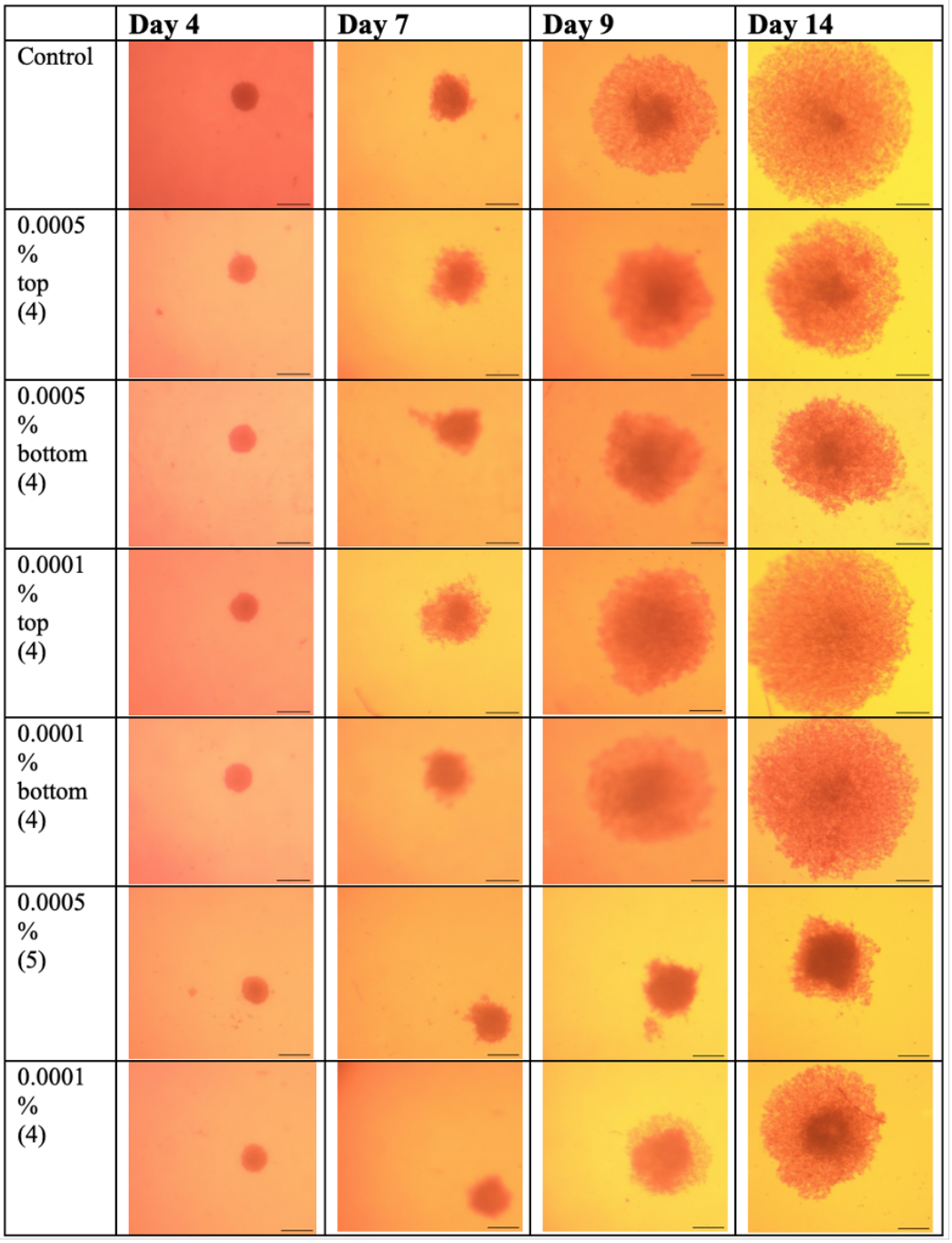


**Figure 4.10:** Differing GrowDex concentrations with a cell density of 2000 cells/well. Scale bar corresponds to 400 µm.

The control groups of both experiments illustrated a decrease in growth over time (Figures 4.11 and 4.12). GrowDex addition after centrifugation did not display stable growth over time. However, GrowDex addition before cell clustering displayed increasing growth levels

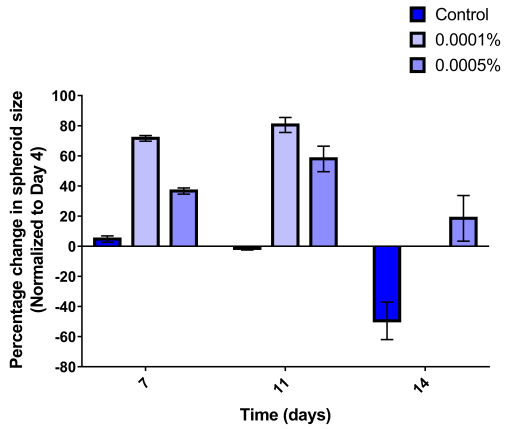


**Figure 4.11:** Relative spheroid growth rate for 2000 cell density per well with 0.0005% and 0.0001% GrowDex concentrations. GrowDex was added 4 days after cell cluster formation

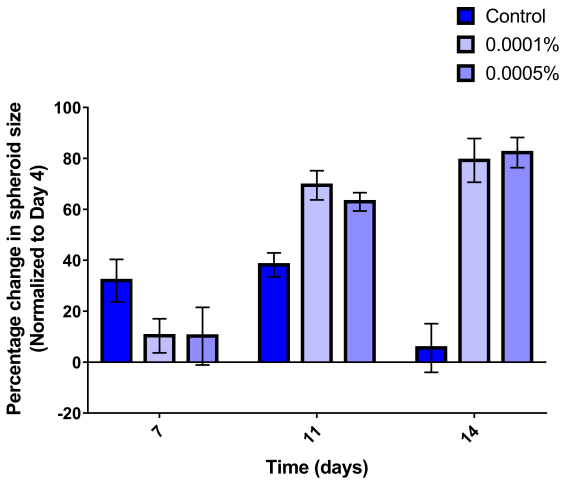


**Figure 4.12:** Relative spheroid growth rate for 2000 cell density per well with 0.0005% and 0.0001% GrowDex concentrations. GrowDex was added 4 days after cell cluster formation

**Cell seeding density of 5000 cells/well**

At 5000 cell seeding density, the control group illustrated relatively stable spheroids, though an increasing monolayer of single cells could be observed (Figure 4.13). Concentrations of 0.0005% illustrated relatively stable spheroids. On the contrary, 0.0001% looked quite similar to the control group, with an increasing monolayer of single cells surrounding the spheroids.

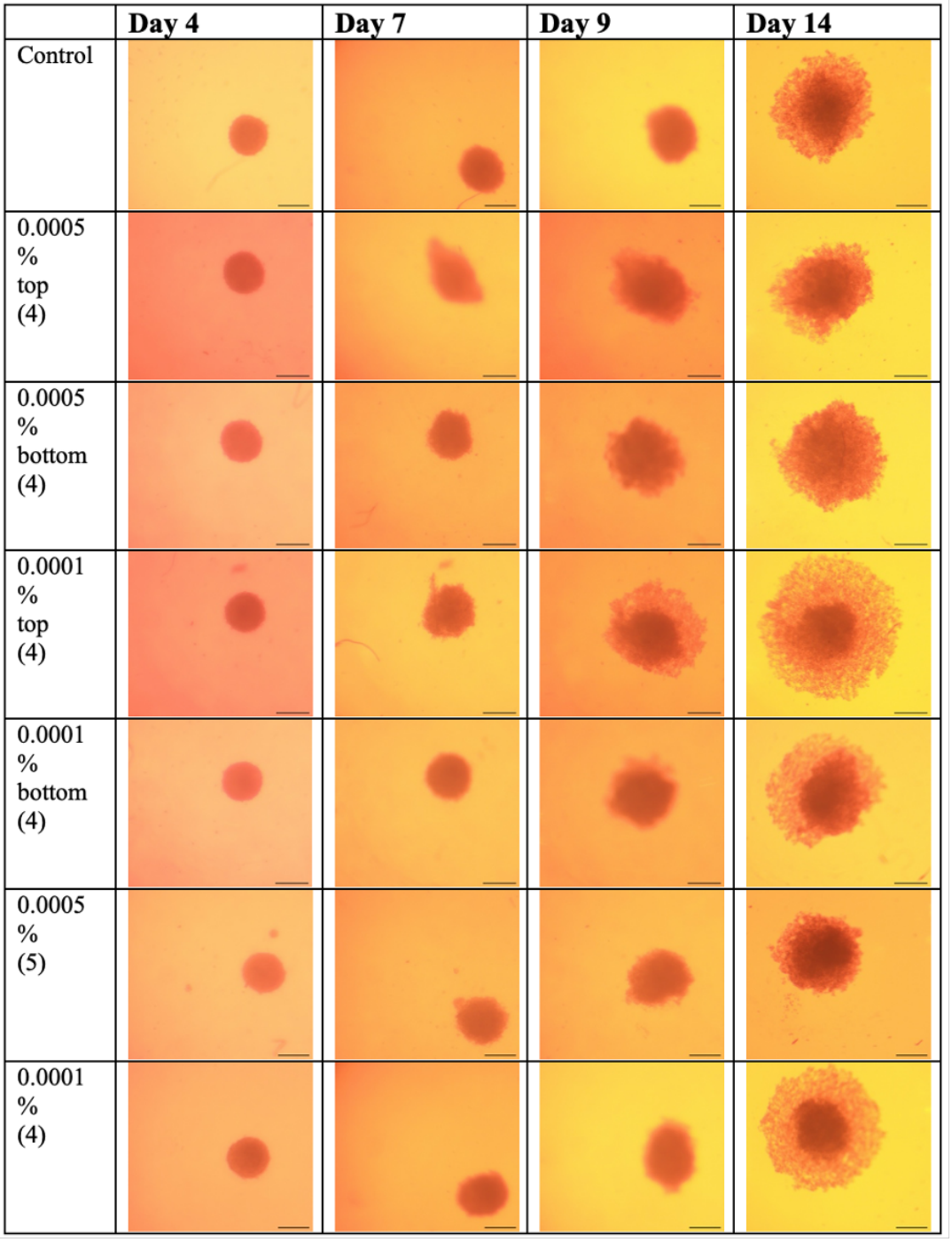


**Figure 4.13:** Differing GrowDex concentrations with a cell density of 5000 cells/well. Scale bar corresponds to 400 µm.

The control groups of both experiments illustrated a decrease in growth over time (Figures 4.14 and 4.15). While the samples with GrowDex addition prior to cell cluster formation illustrated an increase in size followed by a decrease of growth (figure 4.14), the samples where GrowDex addition took place after cell cluster formation illustrated only an increase in growth (Figure 4.15).

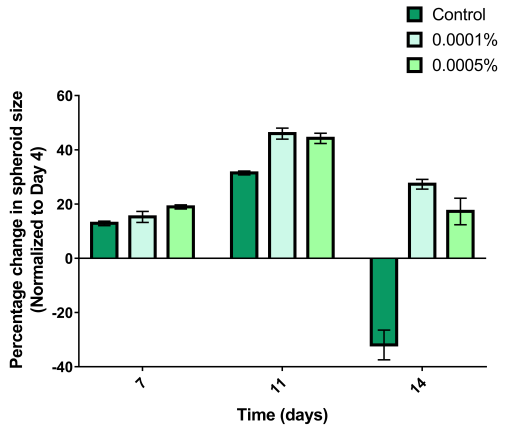


**Figure 4.14:** Relative spheroid growth rate for 5000 cell density per well with 0.0005% and 0.0001% GrowDex concentrations. GrowDex was added 4 days after cell cluster formation

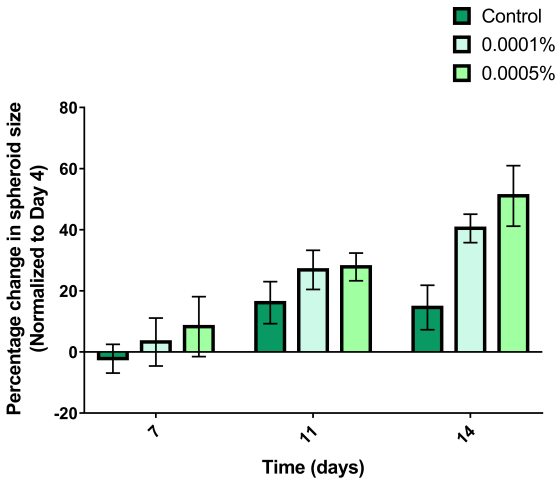


**Figure 4.15:** Relative spheroid growth rate for 5000 cell density per well with 0.0005% and 0.0001% GrowDex concentrations. GrowDex was added 4 days after cell cluster formation

**Cell seeding density of 10000 cells/well**

The control group illustrated familiar behavior, starting out with a single spheroid and eventually developing (an increasing) monolayer of single cells (Figure 4.16). While all the other samples illustrated single spheroids over time, the 0.0001% started to look like the control group over time, while the 0.0005% remained stable (Figure 4.16).

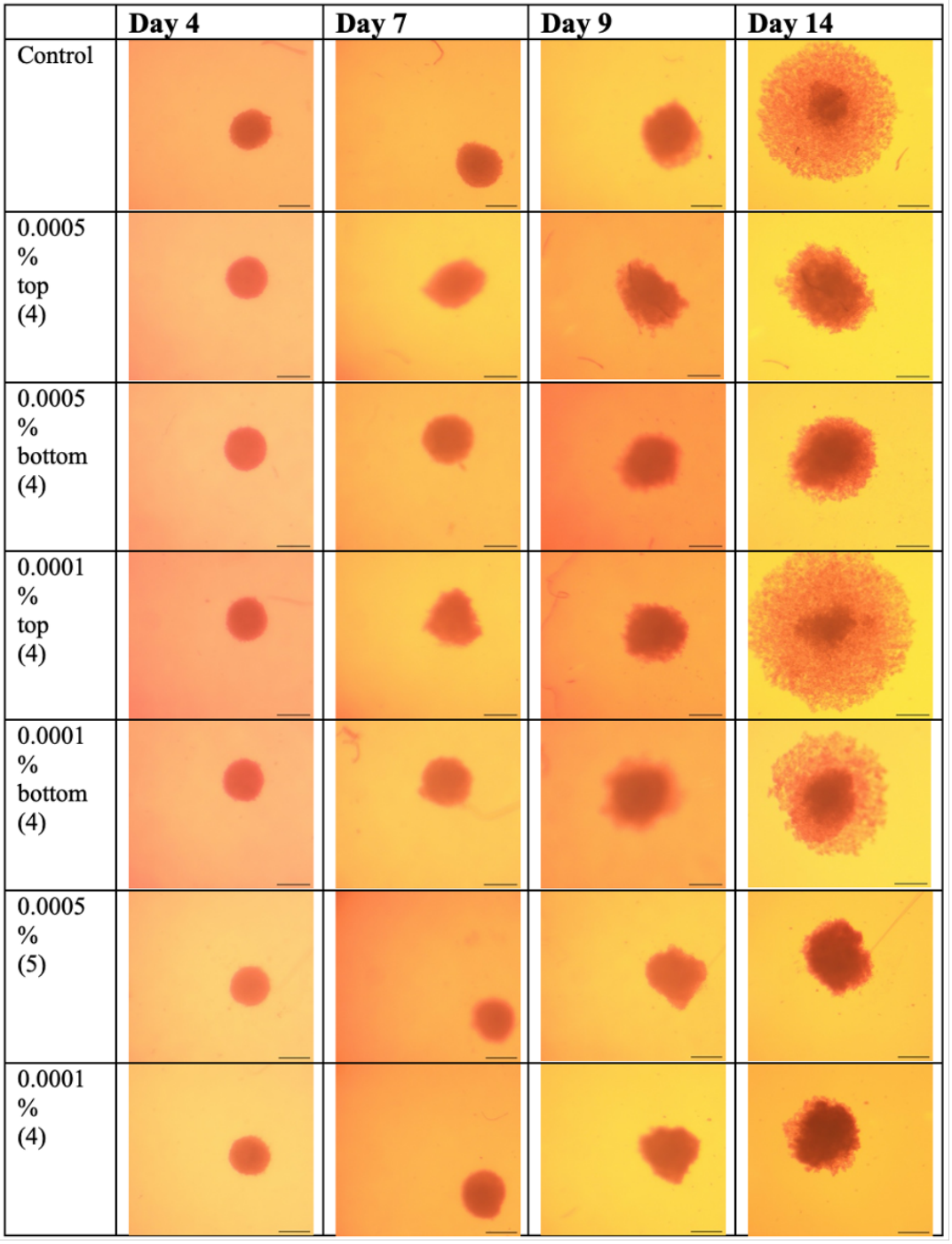


**Figure 4.16:** Differing GrowDex concentrations with a cell density of 10000 cells/well. Scale bar corresponds to 400 µm.

The control groups of both experiments eventually illustrated a decrease in growth, after first illustrating an increase (Figures 4.17 and 4.18). The 0.0001% samples (GrowDex addition after cell cluster formation) illustrated similar behavior as the control group (Figure 4.17), while the 0.0001% samples (centrifugation after GrowDex) only illustrated an increase (Figure 4.18). Furthermore, while the 0.0001% (centrifugation prior to GrowDex addition) illustrated a gradual growth increase (Figure 4.17), the 0.0005% (GrowDex addition prior to cell cluster formation) illustrated an intense growth increase (Figure 4.18).

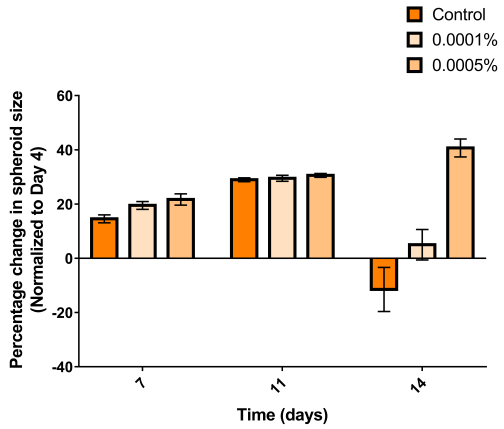


**Figure 4.17:** Relative spheroid growth rate for 10000 cell density per well with 0.0005% and 0.0001% GrowDex concentrations. GrowDex was added 4 days after cell cluster formation

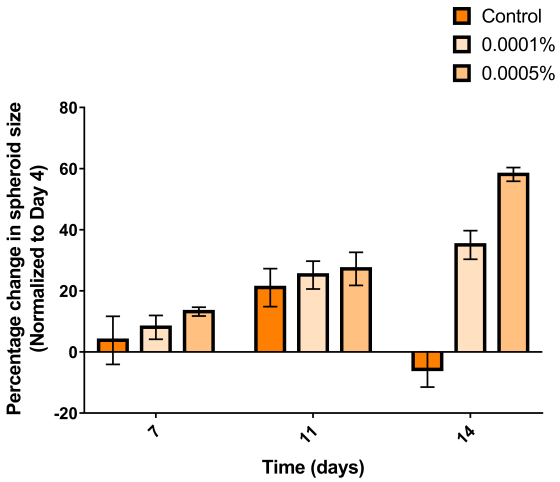


**Figure 4.18:** Relative spheroid growth rate for 10000 cell density per well with 0.0005% and 0.0001% GrowDex concentrations. GrowDex was added 4 days after cell cluster formation

### 4.0.3. ATP viability assay

A CellTiter-Glo3D Cell Viability Assay was performed to confirm the presence of the proliferation zone. within an ideal spheroid.

Figure 4.19 illustrates samples with GrowDex concentrations of 0.001, 0.005, and 0.01%, where GrowDex was added immediately after cell cluster formation. The ATP levels of the samples remained in a similar range of the control groups. For the 2000 cells, the control group was measured at 100%, while the samples were measured between 75-80%. For the 5000 cells, the control group was measured at 80%, while the samples were measured between 65-80%. For the 10000 cells, the control group was measured around 80% as well, while the samples were measured between 55-75%.

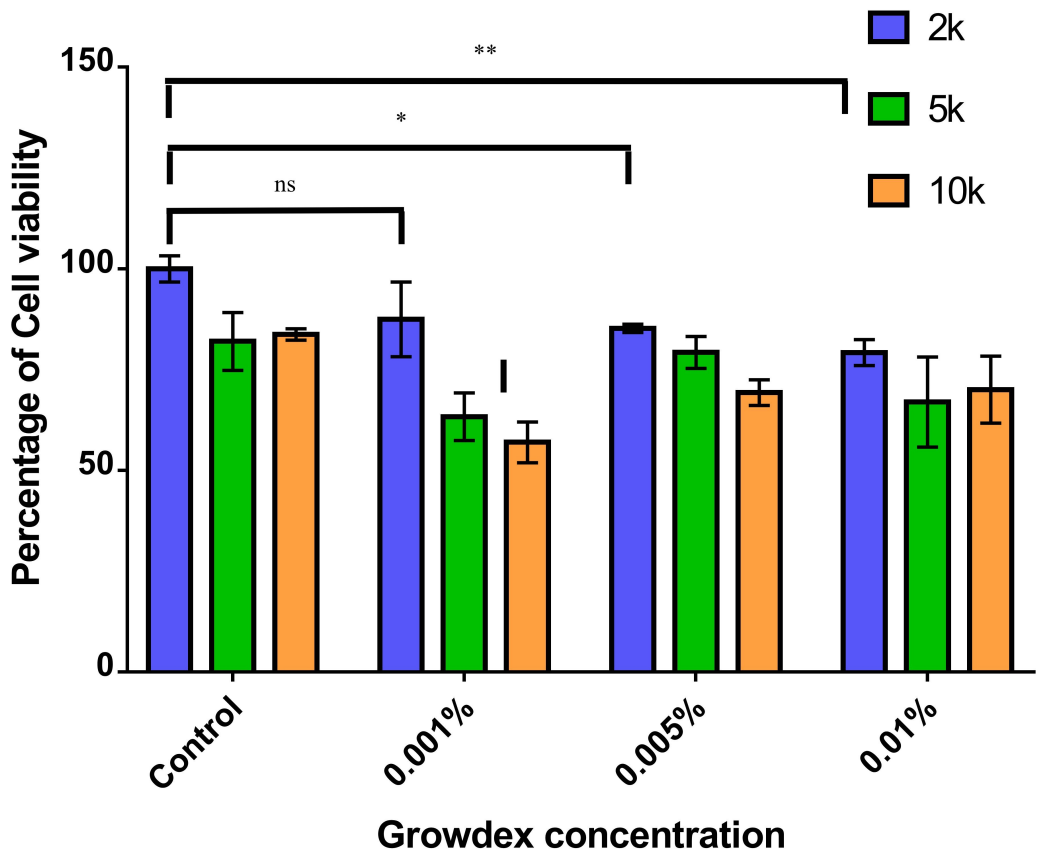


**Figure 4.19:** Cell viability percentage for GrowDex concentrations of 0.001, 0.005 and 0.01%. GrowDex was added immediately after cell cluster formation.

Figure 4.20 illustrates samples with GrowDex concentrations of 0.0001 and 0.0005%, where GrowDex was added 4 days after cell cluster formation. The ATP levels of the 2000 and 5000 samples remained in a similar range of the control groups. For the 2000 cells, the control group was measured at 100%, while the samples were measured around 80%. For the 5000 cells, the control group was measured at 75%, while the samples were measured between 60-80%. For the 10000 cells, the control group was measured around 60%, while the samples were measured between 90-100%.

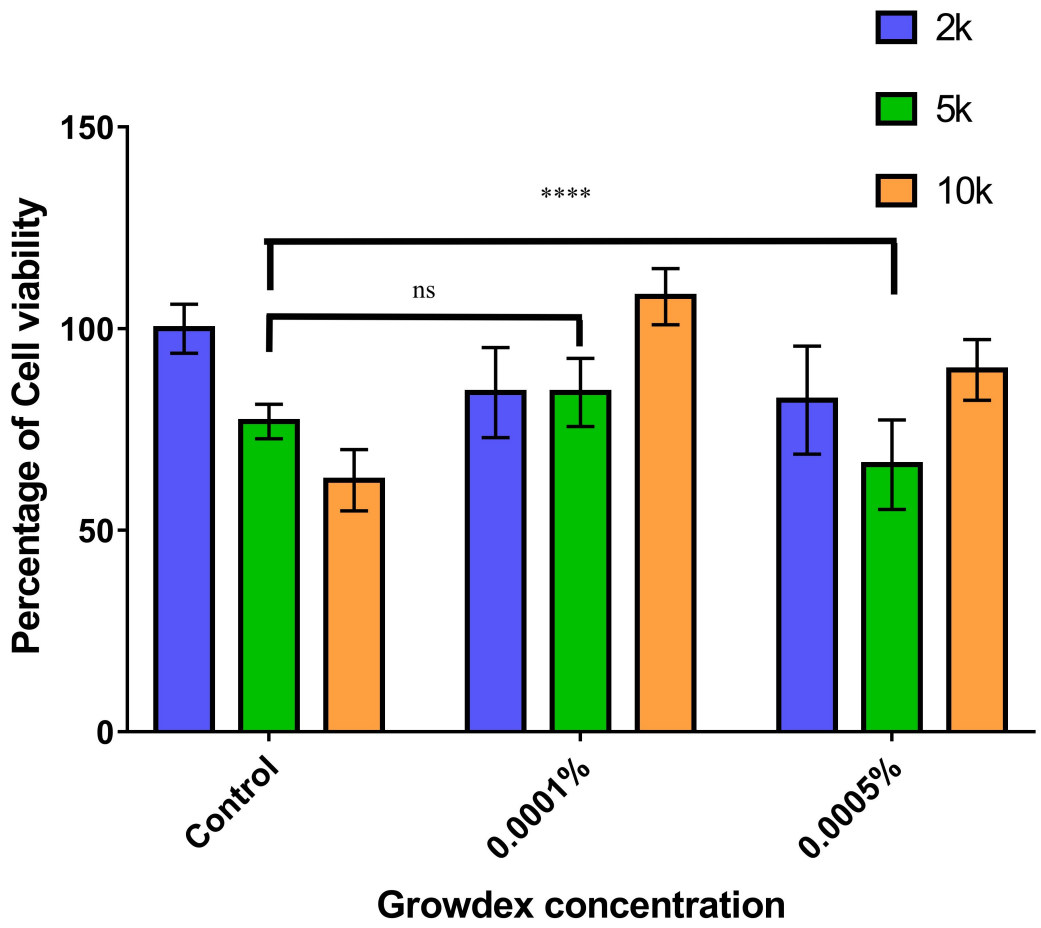


**Figure 4.20:** Cell viability percentage for GrowDex concentrations of 0.0001 and 0.0005%. GrowDex was added 4 days after cell cluster formation.

Figure 4.21 illustrates samples with GrowDex concentrations of 0.0001, 0.0005%, where GrowDex was added prior to cell cluster formation. The ATP levels of the 2000 samples decreased (50-60%) compared to the control group (100%). In contrast, the ATP levels of the 5000 cells increased (95-100%) compared to the control group (70%). The ATP levels of the 10000 cells remained in a similar range of the control group (75-80%).

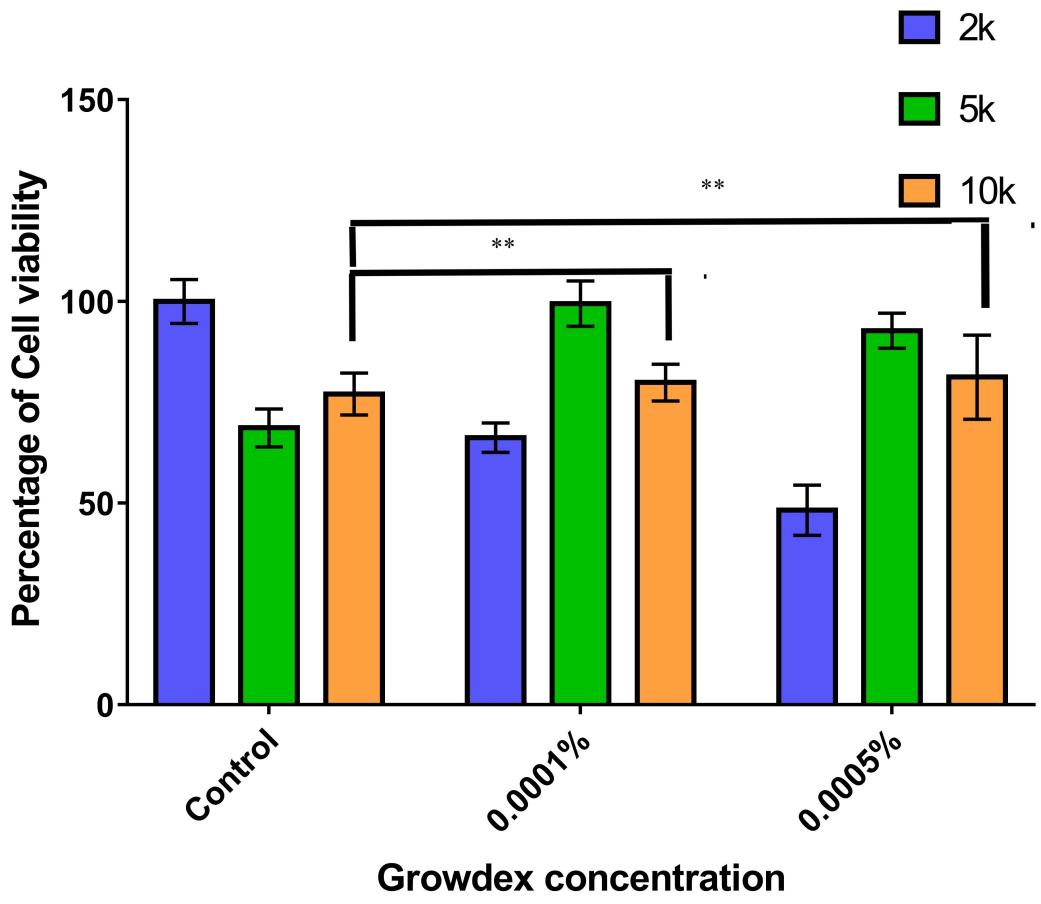


**Figure 4.21:** Cell viability percentage for GrowDex concentrations of 0.0001 and 0.0005%. GrowDex was added prior to cell cluster formation.

# 5

# Discussion

The aim of this research was to determine the optimal conditions for single spheroid formation, employing breast cancer cells and utilizing GrowDex. As GrowDex is solely based on cellulose [30], its viscosity was initially not suitable for spheroid formation. Upon diluting the GrowDex stock however, the viscosity was reduced and GrowDex was found to behave like a scaffold, providing the structural support for spheroid formation.

### 5.0.1. GrowDex concentrations for singular spheroid formation

While single spheroids could initially be detected in all the control groups, after 14 days these spheroids started to disintegrate into a monolayer of single cells surrounding the outer boundaries of the spheroid. This monolayer was found to increase in size over time. Singular spheroid formation for 2000 cells was achieved in 0.1 and 0.05% GrowDex concentrations. Eventhough other concentrations still illustrated an increase in size over time (Figure 4.3), this was due to the observed monolayer of single cells (Figure 4.1), which makes it difficult to characterize the borders of the spheroid. Spheroid growth was also visible in concentrations of 0.0005% and 0.0001%, though this growth reached a plateau state early on (Figures 4.11-12). Singular spheroid formation for 5000 cells was achieved in multiple concentrations as well (Figure 4.13). These concentrations were 0.1, 0.01, 0.0001, and 0.0005% (GrowDex addition prior to cell cluster formation). However, only the 0.1, 0.0001, and 0.0005% illustrated growth until the end of the observation period, while the other concentrations reached a plateau state between day 9-13 (Figures 4.5-6, 4.14-15). Similar to 5000 cells, singular spheroid formation for 10000 cells was achieved in multiple concentrations as well. Increase in growth rate could be observed in concentrations of 0.1, 0.05, 0.01, 0.005, 0.001, 0.0005, and 0.0001%. However, only 0.0001 and 0.0005% (GrowDex addition prior to cell cluster formation) illustrated a consistent increase in growth, with the other concentrations reaching a plateau between day 9-13 (Figures 4.8-9, 4.17-18).

The spheroids reaching a plateau growth rate in certain samples leads to three different theories. The first being that singular spheroid formation had occurred during the earlier days, similar to the control groups. However, the addition of GrowDex after a few days can cause an imbalance and/or disruption in the spheroid microenvironment. This would naturally take the the cells some time to adjust to the new conditions, which might not have been within the scope of observation days of this study. This statement is further strengthened by the fact that even while growth had become stagnant, spheroid disintegration did not occur in the GrowDex samples like it did in the control cells. The second theory is that due to the small concentrations of GrowDex, it is easily possible that the dilutions were not properly mixed. This can cause an inhomogeneous dispersion of GrowDex. Therefore, while GrowDex could still be present and aid stable spheroid formation, it is not present in an ideal distribution, and therefore cannot maximize growth potential. The third theory is that the amount of GrowDex and the applied cell density reaches a saturation point.

To summarize, when working with a cell density of 2000 cells, 0.1 and 0.05% GrowDex are useful. When working with a cell density of 5000 cells, depending on the type of research and its aim, concentrations of 0.1, 0.01, 0.0001, and 0.0005% are useful. For example, when fully grown spheroids are required, it is better to use the concentrations that encourage a growth plateau early on. Whereas concentrations that encourage long-term growth can be useful for other treatment therapies. When

working with 10000 cells, again multiple concentrations are useful. These consist of 0.1, 0.05, 0.01, 0.005, 0.001, 0.0005, and 0.0001%. Similar to the 5000 cells, the ideal concentration depends on the aim of the experiment.

Low GrowDex concentrations and high cell seeding densities are found in literature works as well. As illustrated in an experiment by UPMBiomedicals, a GrowDex concentration of 0.37% was used in combination with a cell density of 25000 cells, resulting in multiple spheroid formation [34]. However, during this experiment there is no mention of the cell clustering formation step, which has been proven to be a crucial step for single spheroid formation (Figures 4.11-18). Adding GrowDex prior to cell cluster formation ensures that the cells and GrowDex form a cell cluster in the center of the wells in a well-mixed state. The addition of GrowDex after cell cluster formation caused the GrowDex to sit directly on top of the cells without really interacting with them, ignoring natural gravity. This leads to the conclusion that GrowDex' viscosity is so dense, even in small dilutions, that it does not interact with cells on its own.

### 5.0.2. Viability assay

During almost all the experiments, the ATP levels of the GrowDex samples were either similar or higher compared to the control samples (Figures 4.19-21). For a cell density of 2000 cells, GrowDex concentrations of 0.0001, 0.0005, 0.001, 0.005, and 0.01% illustrated a good level of live cells. A cell density of 5000 cells and GrowDex concentrations of 0.0001 and 0.0005% (GrowDex addition after to cell cluster formation) illustrated the highest ATP levels compared to controls, while for a cell density of 10000 cells of 0.0001 and 0.0005% (GrowDex addition prior to cell cluster formation) illustrated the highest levels of ATP compared to the controls.

However, as previously mentioned, GrowDex addition after cell cluster formation makes it unlikely for GrowDex to interact with the cells. The high ATP levels of the 5000 cells is therefore unrelated to the spheroids. Figure 4.13 strengthens this statement, as samples where GrowDex addition took place after cell cluster formation (4), could be seen with almost only single cells.

However, in the spheroid samples the presence of a proliferation zone corresponding to active cells could be confirmed due to the previously mentioned ATP levels. This offers a promising outlook for cancer research therapies on multiple fronts.

# 6

# Concluding remarks and recommendations

As GrowDex is an animal-free hydrogel with a completely known composition [30], therapy studies with more variables can be conducted. Furthermore, this type of 3D methodology can decrease the use of laboratory animals.

The methodology of GrowDex prevents a few major drawbacks of common 3D spheroid cultures, that of complex and expensive arrays, and the lack of mechanical stability [8][11]. As very small dilutions of GrowDex are necessary, this product is economically profitable compared to other hydrogels requiring higher concentrations. The application is straight-forward, and the scaffold-like behavior of the GrowDex can create mechanical stability. However, similar to general spheroids, it is difficult to generate spheroids with a uniform size distribution [16]. Though in the case of GrowDex this might just be due to the previously mentioned inhomogeneous dispersion, seeing as the concentrations are so small. Ensuring the GrowDex dilutions are well-mixed could omit this problem all-together.

Low GrowDex concentrations have a positive effect on single spheroid formation when using the MDA-MB-231 breast cancer cell line. However, as the GrowDex concentrations are extremely low, ensuring a homogeneous dispersion is crucial.

Based on the results of this study, the control groups started to illustrate a monolayer of single cells, which would increase over time. Not only would it become difficult to establish the boundaries of the spheroids for growth determination, the spheroids actually became smaller while the monolayer increased. Based on this, the control groups will probably illustrate only single cells after 3 weeks and it would be interesting to see if or when this point will be reached compared to GrowDex samples. This might lead to spheroids being useful for long-term studies.

Lastly, experiments where single spheroid formation using GrowDex is performed in parallel to using other hydrogels could help to increase the knowledge on GrowDex behavior.

# Bibliography


[1] *Worldwide cancer data | World Cancer Research Fund International*. 2020. URL: https://www.wcrf.org/dietandcancer/worldwide-cancer-data/.

[2] Nasrindokht Azamjah, Yasaman Soltan-Zadeh, and Farid Zayeri. "Global Trend of Breast Cancer Mortality Rate: A 25-Year Study". In: *Asian Pacific Journal of Cancer Prevention : APJCP* 20.7 (2019), p. 2015. ISSN: 2476762X. DOI: 10.31557/APJCP.2019.20.7.2015. URL: /pmc/articles/PMC6745227/%20/pmc/articles/PMC6745227/?report=abstract%20https://www.ncbi.nlm.nih.gov/pmc/articles/PMC6745227/.

[3] Nadia Harbeck et al. "Breast cancer". In: *Nature Reviews Disease Primers 2019 5:1* 5.1 (Sept. 2019), pp. 1–31. ISSN: 2056-676X. DOI: 10.1038/s41572-019-0111-2. URL: https://www.nature.com/articles/s41572-019-0111-2.

[4] Ismail Jatoi and Anthony B. Miller. "Why is breast-cancer mortality declining?" In: *The Lancet Oncology* 4.4 (Apr. 2003), pp. 251–254. ISSN: 1470-2045. DOI: 10.1016/S1470-2045(03)01037-4.

[5] *BRCA Gene Mutations: Cancer Risk and Genetic Testing Fact Sheet - NCI*. URL: https://www.cancer.gov/about-cancer/causes-prevention/genetics/brca-fact-sheet.

[6] *What Happens When Cancer Spreads to Lymph Nodes?* URL: https://www.healthline.com/health/what-happens-when-cancer-spreads-to-the-lymph-nodes#cancer-in-lymph-nodes.

[7] *Types of Breast Cancer - National Breast Cancer Foundation*. URL: https://www.nationalbreastcancer.org/types-of-breast-cancer/.

[8] *Triple-negative Breast Cancer | Details, Diagnosis, and Signs*. URL: https://www.cancer.org/cancer/breast-cancer/about/types-of-breast-cancer/triple-negative.html.

[9] Jo Ellen Welsh. "Animal Models for Studying Prevention and Treatment of Breast Cancer". In: *Animal Models for the Study of Human Disease* (Jan. 2013), pp. 997–1018. DOI: 10.1016/B978-0-12-415894-8.00040-3.

[10] "Cell line profile MDA-MB-231 (ECACC catalogue no. 92020424)". In: ().

[11] Tao Jiang et al. "Directing the Self-assembly of Tumour Spheroids by Bioprinting Cellular Heterogeneous Models within Alginate/Gelatin Hydrogels". In: *Scientific Reports 2017 7:1* 7.1 (July 2017), pp. 1–9. ISSN: 2045-2322. DOI: 10.1038/s41598-017-04691-9. URL: https://www.nature.com/articles/s41598-017-04691-9.

[12] Gabrielle Wishart et al. "3d tissue models as tools for radiotherapy screening for pancreatic cancer". In: *British Journal of Radiology* 94.1120 (Apr. 2021), p. 20201397. ISSN: 1748880X. DOI: 10.1259/BJR.20201397/ASSET/IMAGES/LARGE/BJR.20201397.G003.JPEG. URL: https://www.birpublications.org/doi/full/10.1259/bjr.20201397.

[13] Kathleen A. Fitzgerald et al. "Life in 3D is never flat: 3D models to optimise drug delivery". In: *Journal of Controlled Release* 215 (Oct. 2015), pp. 39–54. ISSN: 0168-3659. DOI: 10.1016/J.JCONREL.2015.07.020.

[14] Donglai Lv et al. "Three-dimensional cell culture: A powerful tool in tumor research and drug discovery". In: *Oncology Letters* 14.6 (Dec. 2017), pp. 6999–7010. ISSN: 17921082. DOI: 10.3892/OL.2017.7134/HTML. URL: http://www.spandidos-publications.com/10.3892/ol.2017.7134/abstract%20https://www.spandidos-publications.com/10.3892/ol.2017.7134.

[15] Roghayyeh Baghban et al. "Tumor microenvironment complexity and therapeutic implications at a glance". In: *Cell Communication and Signaling 2020 18:1* 18.1 (Apr. 2020), pp. 1–19. ISSN: 1478-811X. DOI: 10.1186/S12964-020-0530-4. URL: https://biosignaling.biomedcentral.com/articles/10.1186/s12964-020-0530-4.

[16] Elisabete C. Costa et al. “3D tumor spheroids: an overview on the tools and techniques used for their analysis”. In: *Biotechnology Advances* 34.8 (Dec. 2016), pp. 1427–1441. ISSN: 0734-9750. DOI: 10.1016/J.BIOTECHADV.2016.11.002.

[17] Sarah C. Brüningk et al. “3D tumour spheroids for the prediction of the effects of radiation and hyperthermia treatments”. In: *Scientific Reports* 10.1 (Dec. 2020). ISSN: 20452322. DOI: 10.1038/S41598-020-58569-4.

[18] Khashayar Moshksayan et al. “Spheroids-on-a-chip: Recent advances and design considerations in microfluidic platforms for spheroid formation and culture”. In: *Sensors and Actuators B: Chemical* 263 (June 2018), pp. 151–176. ISSN: 0925-4005. DOI: 10.1016/J.SNB.2018.01.223.

[19] Se Jik Han, Sangwoo Kwon, and Kyung Sook Kim. “Challenges of applying multicellular tumor spheroids in preclinical phase”. In: *Cancer Cell International 2021 21:1* 21.1 (Mar. 2021), pp. 1–19. ISSN: 1475-2867. DOI: 10.1186/S12935-021-01853-8. URL: https://cancerci.biomedcentral.com/articles/10.1186/s12935-021-01853-8.

[20] Andrea Ivascu and Manfred Kubbies. “Rapid Generation of Single-Tumor Spheroids for High-Throughput Cell Function and Toxicity Analysis”. In: *SLAS Discovery* 11.8 (Dec. 2006), pp. 922–932. ISSN: 2472-5552. DOI: 10.1177/1087057106292763.

[21] Karolin Froehlich et al. “Generation of Multicellular Breast Cancer Tumor Spheroids: Comparison of Different Protocols”. In: *Journal of Mammary Gland Biology and Neoplasia* 21.3-4 (Dec. 2016), pp. 89–98. ISSN: 15737039. DOI: 10.1007/S10911-016-9359-2/FIGURES/4. URL: https://link.springer.com/article/10.1007/s10911-016-9359-2.

[22] Chungmin Han, Shuichi Takayama, and Jaesung Park. “Formation and manipulation of cell spheroids using a density adjusted PEG/DEX aqueous two phase system”. In: *Scientific Reports 2015 5:1* 5.1 (July 2015), pp. 1–12. ISSN: 2045-2322. DOI: 10.1038/srep11891. URL: https://www.nature.com/articles/srep11891.

[23] *Problems with Animal Research - American Anti-Vivisection Society*. URL: https://aavs.org/animals-science/problems-animal-research/.

[24] Mariana R. Carvalho et al. “Evaluating Biomaterial- and Microfluidic-Based 3D Tumor Models”. In: *Trends in Biotechnology* 33.11 (Nov. 2015), pp. 667–678. ISSN: 0167-7799. DOI: 10.1016/J.TIBTECH.2015.09.009.

[25] Sophie Roberts, Sally Peyman, and Valerie Speirs. “Current and Emerging 3D Models to Study Breast Cancer”. In: *Advances in Experimental Medicine and Biology* 1152 (2019), pp. 413–427. ISSN: 22148019. DOI: 10.1007/978-3-030-20301-6{_}22/FIGURES/4. URL: https://link.springer.com/chapter/10.1007/978-3-030-20301-6_22.

[26] Ibrahim T. Ozbolat. “Scaffold-Based or Scaffold-Free Bioprinting: Competing or Complementing Approaches?” In: *Journal of Nanotechnology in Engineering and Medicine* 6.2 (May 2015). ISSN: 19492952. DOI: 10.1115/1.4030414/376811. URL: https://asmedigitalcollection.asme.org/nanoengineeringmedical/article/6/2/024701/376811/Scaffold-Based-or-Scaffold-Free-Bioprinting.

[27] Susan Breslin and Lorraine O’Driscoll. “Three-dimensional cell culture: the missing link in drug discovery”. In: *Drug Discovery Today* 18.5-6 (Mar. 2013), pp. 240–249. ISSN: 1359-6446. DOI: 10.1016/J.DRUDIS.2012.10.003.

[28] Esra Türker, Nida Demirçak, and Ahu Arslan-Yildiz. “Scaffold-free three-dimensional cell culturing using magnetic levitation”. In: *Biomaterials Science* 6.7 (June 2018), pp. 1745–1753. ISSN: 20474849. DOI: 10.1039/C8BM00122G. URL: https://pubs.rsc.org/en/content/articlehtml/2018/bm/c8bm00122g%20https://pubs.rsc.org/en/content/articlelanding/2018/bm/c8bm00122g.

[29] Pujan K. Desai, Hubert Tseng, and Glauco R. Souza. “Assembly of Hepatocyte Spheroids Using Magnetic 3D Cell Culture for CYP450 Inhibition/Induction”. In: *International Journal of Molecular Sciences 2017, Vol. 18, Page 1085* 18.5 (May 2017), p. 1085. ISSN: 1422-0067. DOI: 10.3390/IJMS18051085. URL: https://www.mdpi.com/1422-0067/18/5/1085/htm%20https://www.mdpi.com/1422-0067/18/5/1085.

[30] *How to transfer animal-free from animal-derived matrices | UPM Biomedicals*. URL: https://www.upmbiomedicals.com/for-life-science/transfer-animal-free/.

[31] UPM Biomedicals. *HOW TO TRANSFER from animal-derived matrices to GrowDex-3D cell culture matrix Contents*. URL: https://www.upmbiomedicals.com/for-life-science/growdex-hydrogels/growdex-offer/#cid_362389.

[32] N. Oridate, R. Lotan, and D. Lotan. "Reconstituted basement membrane (matrigel®): A useful semisolid medium for growth of tumor cell colonies". In: *In Vitro Cellular & Developmental Biology - Animal 1996 32:4* 32.4 (1996), pp. 192–193. ISSN: 1543-706X. DOI: 10.1007/BF02722944. URL: https://link.springer.com/article/10.1007/BF02722944.

[33] *Cell Viability Guide | How to Measure Cell Viability*. URL: https://nld.promega.com/resources/guides/cell-biology/cell-viability/.

[34] Johanna Niklander and Lauri Paasonen. *Breast Cancer Cell Line MCF7 3D Culture Demonstrated in GrowDex ® and Matrigel*. 2019. URL: https://www.upmbiomedicals.com/siteassets/documents/application-notes/growdex-application-note-29.pdf.